BIOCHEMICAL AND BIOPHYSICAL RESEARCH COMMUNICATIONS **246,** 39–44 (1998)
ARTICLE NO. RC988566

Identification of a Potential Substrate Binding Domain in the Mammalian Peptide Transporters PEPT1 and PEPT2 Using PEPT1-PEPT2 and PEPT2-PEPT1 Chimeras

You-Jun Fei, Jin-Cai Liu, Takuya Fujita, Rong Liang, Vadivel Ganapathy, and Frederick H. Leibach[1]

Department of Biochemistry and Molecular Biology, Medical College of Georgia, Augusta, Georgia 30912-2100

Received March 19, 1998

The mammalian peptide transporters PEPT1 and PEPT2 are energized by a transmembrane electrochemical H^+ gradient and exhibit similar broad substrate specificity. These transporters however differ in their affinity for substrates, PEPT1 being a low-affinity transporter and PEPT2 being a high-affinity transporter. To identify the substrate binding domain in PEPT1 and PEPT2 which is responsible for the differing affinities, we constructed a series of PEPT1-PEPT2 and PEPT2-PEPT1 chimeras using an *in vivo* restriction site-independent procedure and determined their substrate affinities. A comparison of these kinetic data for different chimeras with those of the wild-type PEPT1 and PEPT2 in conjunction with the specific structural PEPT1/PEPT2 crossover regions in these chimeras has led to the identification of a putative substrate binding site, which is comprised of the transmembrane domains 7, 8 and 9 of the transporters.

Mammalian peptide transporters (PEPTs) play an important role in the absorption and reclamation of small peptides in the epithelial cells of intestinal tract and kidney tubules (1-3). A comprehensive knowledge concerning the structure and function of the PEPTs has been obtained in recent years through biochemical and molecular biological studies (4, 5). These studies have led to the identification of two distinct peptide transporters, PEPT1 and PEPT2, expressed in the intestine and kidney (6-13). These transporters are unique in mammalian systems due to their dependence on a transmembrane H^+ gradient rather than a Na^+ gradient as the driving force. In addition to their natural substrates, the mammalian PEPTs are also capable of transporting several pharmacologically active compounds including β-lactam antibiotics, the antitumor agent bestatin, angiotensin converting enzyme inhibitors, and renin inhibitors (1-5). The potential for nutritional, clinical, and therapeutic applications of the PEPTs necessitates a clear understanding of the molecular aspects of the carrier proteins responsible for this process.

PEPT1 as well as PEPT2 possess 12 transmembrane domains (TMD) and exhibit significant homology at the level of amino acid sequence. The amino acid sequence in the intra- or extracellular loops is more divergent than that in the putative TMDs (4). Functionally, PEPT1 and PEPT2 have very similar substrate specificity, recognizing a wide variety of di-, tri- and teterapeptides. However, kinetic analysis has revealed that PEPT1 and PEPT2 differ in their affinity for the peptide substrates, the former being a low-affinity type and the latter a high-affinity type. This difference in the substrate affinity is likely to be a result of variations in the structure of the substrate binding domain of the two transporters.

To identify the putative substrate binding domain in PEPT1 and PEPT2, we generated a series of PEPT1–PEPT2 and PEPT2–PEPT1 chimeras and analyzed their substrate affinities. These studies have demonstrated that the putative substrate binding domain in PEPT1 as well as in PEPT2 lies in the region which is comprised of the TMDs 7, 8, and 9.

MATERIALS AND METHODS

"Head-to-tail" tandem dimer construction containing both hPEPT1 and rPEPT2 cDNA inserts. We used an *in vivo* restriction site-independent procedure to generate PEPT1–PEPT2 and PEPT2–PEPT1 chimeras. This method was originally described for the construction of adenylate cyclase chimeras (14) and subsequently applied successfully for the construction of chimeras of monoamine transporters (15, 16). To prepare recipient plasmid DNA, the hPEPT1 plasmid DNA (pBluescript-based) was double-digested with unique cutters, *Not*I and *Sma*I. The rPEPT2 plasmid DNA (pSPORT-based), was also digested with the same restriction enzymes. The *Sma*I restriction site is located on the 5′-end within the vector

[1] Corresponding author. Fax: 706-721-6608.

0006-291X/98 $25.00

(pSPORT). Here, we took advantage of the differential distribution of the restriction sites in the parental plasmid DNAs. The 3.9 kb *Not*I/*Sma*I donor fragment from rPEPT2 was gel-purified, and ligated to the hPEPT1 recipient DNA fragment to create a T7-hPEPT1-rPEPT2 dimer in which the dimer insert is located downstream of the T7 promoter in the pBluescript vector. A similar procedure was used to create another dimer (T7-rPEPT2-hPEPT1) of opposite orientation with respect to hPEPT1 and rPEPT2 in the pBluescript vector. The 3.9 kb donor fragment from rPEPT2 was prepared by *Sal*I and *Sna*BI double-digestion; the recipient plasmid DNA was generated by *Sal*I and *Pml*I double-digestion of plasmid hPEPT1. Both *Sna*BI and *Pml*I are the blunt-end cutters and created compatible ends in the donor and the recipient for ligation. Transformation and plasmid isolation were performed according to a standard procedure (16).

Dimer linearization and transformation. A unique cutter, *Sma*I, located between hPEPT1 and rPEPT2 in the T7-hPEPT1-rPEPT2 dimer, was selected to linearize this construct. Similarly, a unique cutter *Pfl*II, located beteeen rPEPT2 and hPEPT1 in the T7-rPEPT2-hPEPT1 dimer, was used to linearize this construct. Following the linearization of the dimers, the DNA was dephosphorylated with calf intestinal alkaline phosphatase (Promega, Madison, WI) to avoid recircularization in the subsequent transformation procedure. Maxi DH10B competent cells (Gibco, BRL, Gaithersburg, MD) were used as a host strain for the heat-shock transformation protocol. Bacteria culture and plasmid DNA preparation followed a standard protocol (16). Potential monomeric clones were selected by 0.8% agarose gel electrophoresis and their sizes compared with a standard supercoiled plasmid DNA ladder (Gibco, BRL, Gaithersburg, MD) electrophoresed in parallel. Diagnostic restriction enzyme digestion was performed to predict different switch points in the recombinant monomers. The precise crossover points were confirmed by DNA sequencing performed in an automatic DNA sequencer (Applied Biosystems, Foster City, CA).

Screening of the chimeric cDNA library. Potential monomeric clones were screened for their transport activity in a vaccinia/T7 expression system as described previously (8, 9). In brief, subconfluent HeLa cells were first infected with a recombinant (VTF_{7-3}) vaccinia virus encoding the T7 RNA polymerase and then transfected with the monomer plasmid DNAs. After 8-10 hours post-transfection, transport measurements were made with [2-^{14}C]glycyl-[1-^{14}C]-sarcosine (Gly-Sar, specific radioactivity 109 mCi/mmol, Cambridge Research Biochemicals, Wilmington, DE). The uptake medium was 25 mM Mes/Tris (pH 6.0) containing 140 mM NaCl, 5.4 mM KCl, 1.8 mM $CaCl_2$, 0.8 mM $MgSO_4$ and 5 mM glucose. A negative control (HeLa cells transfected with the pBluescript vector alone) and a positive control (HeLa cells transfected with pBluescript hPEPT1 cDNA) were always included for comparison.

cRNA preparation and oocyte injection. In vitro transcription of the chimeric plasmid DNA was performed after linearization of the template DNA by a restriction endonuclease (*Not*I) digestion at a downstream position from the 3′-end of the poly(A) tail. The transcription was carried out using bacteriophage T7 RNA polymerase. RNAase inhibitor and mRNA cap analog (7-methyldiguanosine triphosphate [mG(5′)ppp(5′)G] were included. cRNA capping was achieved simultaneously by including the mRNA cap analog (Ambion Inc., Austin, TX). The DNA template in the reaction mixture was removed by digestion with an RNase-free DNase following the *in vitro* transcription. Final concentration of the synthetic cRNA was adjusted based on quantification by UV spectrophotometry and the integrity was verified by electrophoresis.

Oocytes, isolated from *Xenopus laevis* (Nasco, Fort Atkinson, WI), were subjected to a partial digestion with collagenase A, 1.6 mg/ml (Boehringer Mannheim, Indianapolis, IN), in a calcium-free buffer for 30 minutes at room temperature, and manually defolliculated. Defolliculated mature (stage V-VI) oocytes were selected and maintained at 18°C in modified Barth's medium with 10 μg/μl gentamicin sulfate. Oocytes were injected 1 day after isolation with approximately 50 ng of the cRNA derived from the plasmid DNA encoding the parental or chimeric peptide transporters, and incubated at 18°C until the experiment was carried out as previously described (6, 17, 18).

Electrophysiologic studies. Conventional two-microelectrode voltage clamp (TEVC) method was used to study the kinetics of the peptide transporters expressed in oocytes. The membrane potential was clamped at −50 mV as previously described (6, 17, 18). Electrophysiologic measurements were made 5-10 days after injection. A standard transport assay buffer (100 mM NaCl-2 mM KCl-1 mM $MgCl_2$-1 mM $CaCl_2$-3 mM HEPES-3 mM MES-3mM Tris, pH 5.5) was used as the bath solution. The recording chamber was perifused with the bath solution and the testing substrates, applied at the desired concentration. Acquired data were fitted to the following equation, $I = I_{max}(S)^n/[(K_{0.5})^n + (S)^n]$, where I is the substrate-evoked current, I_{max} is the derived current maximum, [S] is the substrate concentration applied, n is the Hill coefficient, and $K_{0.5}$ is the Michaelis-Menten constant, or the substrate concentration at which current is half-maximal (17, 18). Kinetic analyses were performed using the software SigmaPlot (Jandel Scientific, San Rafael, CA). Substrates were purchased from Sigma (St. Louis, MO).

To investigate the membrane potential dependence of the transporter activity, step changes to the testing potentials (V_t) from the holding potential (V_h) were achieved by a voltage clamp amplifier (GeneClamp 500, Axon Instruments, CA) controlled by the Clampex computer program of pCLAMP software version 6.0 (Axon Instruments, CA), each for a duration of 100 ms (from +50 mV to −150 mV in 20 mV increments). First, the voltage-jumping protocol was applied in a substrate-free solution, then after superfusing 2-5 minutes, with the test solutions. The substrate-induced current at each test potential was taken as the difference between the steady-state currents, recorded at the end of each voltage pulse, in the presence and absence of the substrate. The current was low pass filtered at 500 Hz by a built-in Bessel filter in the amplifier, digitized at 50 μs/point, and were averaged from three sweeps (6, 17, 18).

RESULTS AND DISCUSSION

hPEPT1 exhibits robust activity in *Xenopus leavis* oocytes as assessed by electrophysiologic approaches (17, 18). hPEPT2 exhibits severalfold lower activity in the same experimental system. However, rPEPT2 which we have recently cloned from rat brain has considerably much higher activity than hPEPT2. Therefore, we selected hPEPT1 and rPEPT2 for the generation of chimeras. Two chimeric cDNA libraries with different configurations (T7-hPEPT1-rPEPT2 and T7-rPEPT2-hPEPT1) were established by transformation of the competent cells (DH10B) with linearized parental dimers. Plasmid DNA was prepared from the transformants. The potential *in vivo* monomerization was determined by a rapid mini-gel electrophoresis method using a supercoiled plasmid DNA standard as a size marker. The *in vivo* monomer formation efficiency ranged between 10 and 30% in different transformation experiments. Approximately 30–40 monomers from each chimeric cDNA library were selected for assessment of transport function using the vaccinia/T7 expression system. Several clones were found to exhibit transport activity. The crossover point between hPEPT1 and rPEPT2 in these functional chimeras was determined tentatively based upon their unique restriction patterns in the diagnostic test. Fi-

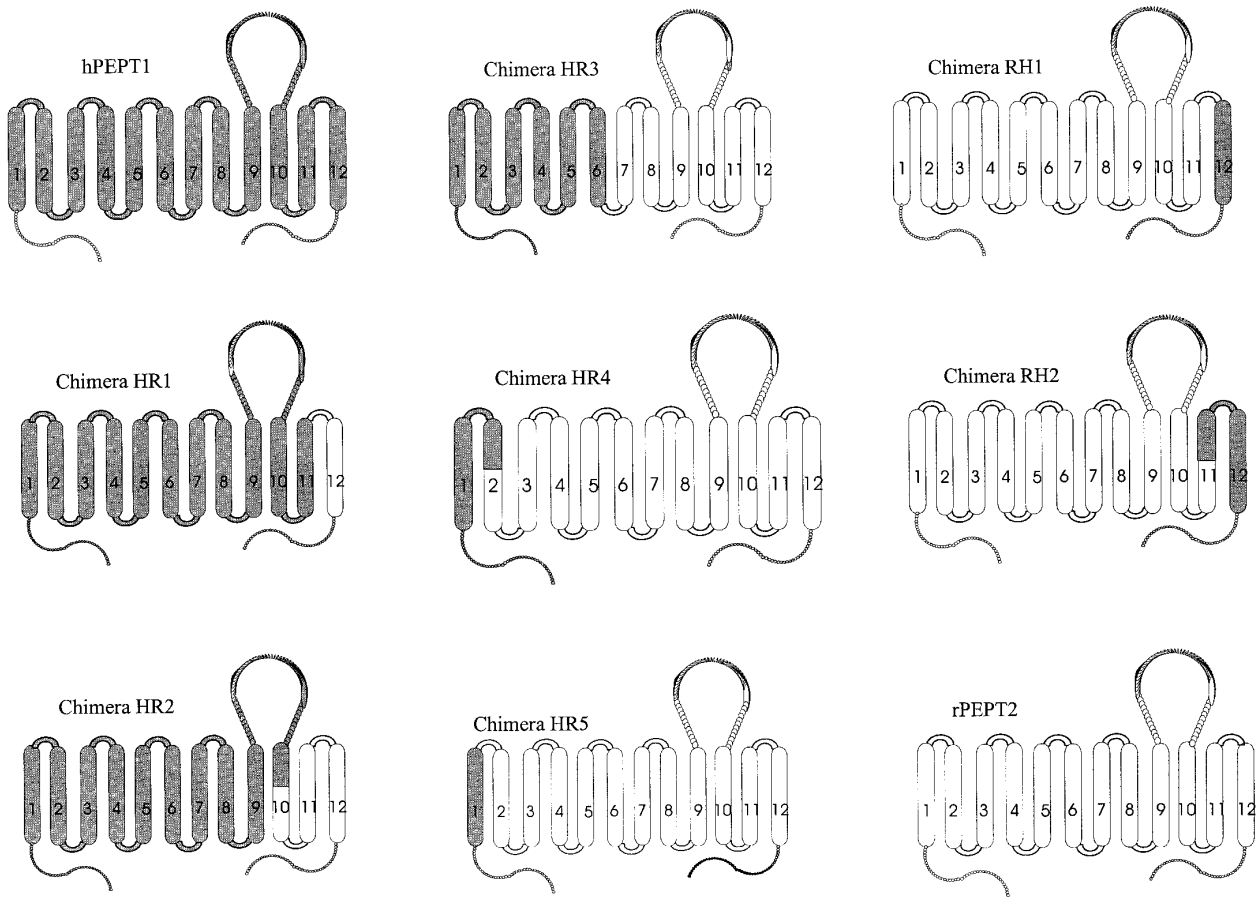

FIG. 1. Chimeric PEPTs composed of different domains derived from the parental hPEPT1 and rPEPT2.

nally, seven clones were selected, five with the T7-hPEPT1-rPEPT2 configuration (designated as HR1, HR2, HR3, HR4 and HR5) and two with the T7-rPEPT2-hPEPT1 configuration (designated as RH1 and RH2) and each of theses clones possessed distinct crossover points. These crossover regions were confirmed by DNA sequencing. Since the crossover regions have a stretch of sequence that is identical to the sequence of the particular regions in hPEPT1 and rPEPT2, the exact crossover points could not be determined. Therefore, the crossover points are arbitrarily assigned in the middle of the amino acid stretches, which could be derived from either of the parental clones (Fig. 1). The N-terminus of the chimeras HR1 through HR5 is composed of the first 11, 92, 6, 12 and 1 transmembrane domains (TMD) with the corresponding intra- and extracellular loops between TMDs derived from hPEPT1, respectively. The rest of TMD and loops are derived from rPEPT2. The C-terminus of the chimeras RH1 and RH2 possesses the last 1 and 12 TMDs derived from hPEPT1, respectively. The remaining portions of these clones are derived from rPEPT2.

A prototypical substrate for peptide transporters, Gly-Sar, was used in the transport kinetic analysis for the engineered multiple chimeric PEPTs. Since the substrate-induced current maximum (I_{max}) in the PEPT-expressing oocytes is not only dependent on transport velocity, but also on the transporter density expressed on the oocyte plasma membrane, we have focused only on the apparent affinity ($K_{0.5}$) in the kinetic analysis. Initial kinetic analysis with TEVC protocol enabled us to categorize the chimeras into two groups according to their apparent affinity for Gly-Sar at pH 5.5. The low-affinity group, chimeras HR1 and HR2, showed an apparent affinity for Gly-Sar ($K^{GS}_{0.5}$), within a range similar to those of hPEPT1 at all the testing membrane potentials from −50 mV to −110 mV. The high-affinity group, chimeras HR3, HR4, HR5, RH1 and RH2, showed $K^{GS}_{0.5}$ values similar to those of rPEPT2. Since the $K^{GS}_{0.5}$ values for all the clones in each group were almost identical, we have chosen chimera HR2 as the representative of the low-affinity group and chimeras HR3 as the representative of the high-affinity group.

Fig. 2 describes the relationship between Gly-Sar concentration and Gly-Sar-induced current at a testing

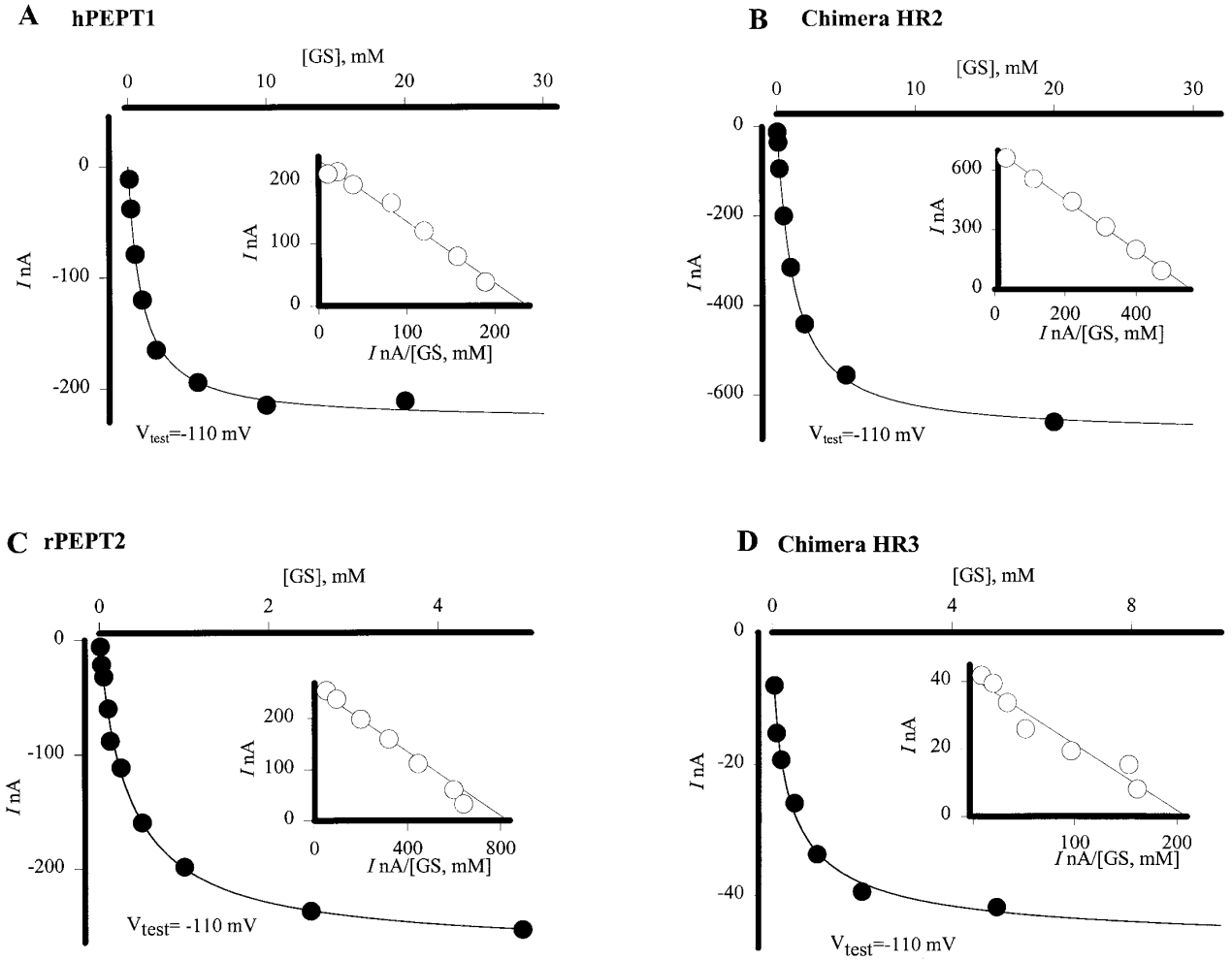

FIG. 2. Substrate-induced currents as a function of the substrate concentration. The substrate (Gly-Sar) induced-currents (*I*) in the PEPT-expressing oocytes are shown as a function of the bath-applied substrate concentrations [GS] at a testing membrane potential (V_{test}), −110 mV. The inserts in each panel are the Eadie-Hofstee transformations of the corresponding data. The apparent affinity for Gly-Sar, $K_{0.5}^{GS}$, was calculated by both non-linear and linear regression methods.

membrane potential of −110 mV for the parental clones hPEPT1 and rPEPT2 and the representatives of the low-affinity group (chimera HR2) and high-affinity group (chimera HR3). In each case, the substrate-induced current was saturable with respect to substrate concentration and the relationship obeyed a transport model describing a single saturable transport system. This was confirmed by nonlinear regression analysis as well as by linear regression analysis. The $K_{0.5}^{GS}$ for hPEPT1 was 1.7 ± 0.1 mM. The corresponding value for chimera HR2, which is the representative of the low-affinity group, was 1.4 ± 0.4 mM. The $K_{0.5}^{GS}$ for rPEPT2 was 0.35 ± 0.04 mM. The corresponding value for chimera HR3, which is the representative of the high-affinity group, was 0.34 ± 0.04 mM. Thus, the substrate affinity of chimera HR2 was similar to that of hPEPT1 whereas the substrate affinity of chimera HR3 was similar to that of rPEPT2.

Since the maximal induced current (I_{max}) varied from oocyte to oocyte due to changes in the level of the heterologous expression of the PEPTs, we normalized the I_{max} for each of these four clones and analyzed the substrate saturation data by the Eadie-Hofstee method (Fig. 3A). It is readily apparent that the slope of the line representing the data for chimera HR2 is almost identical to that of the line representing hPEPT1. Similarly, the slope of the line representing the data for chimera HR3 is nearly the same as that of the line representing rPEPT2. Since the slope of the line provides the $K_{0.5}^{GS}$ value, it is clear that the substrate affinity of chimera HR2 is similar to that hPEPT1 whereas the substrate affinity of chimera HR3 is similar to that of rPEPT2.

We also determined the $K_{0.5}^{GS}$ values for these clones at different testing membrane potentials (−50, −70, −90, and −110 mV). At each of these membrane poten-

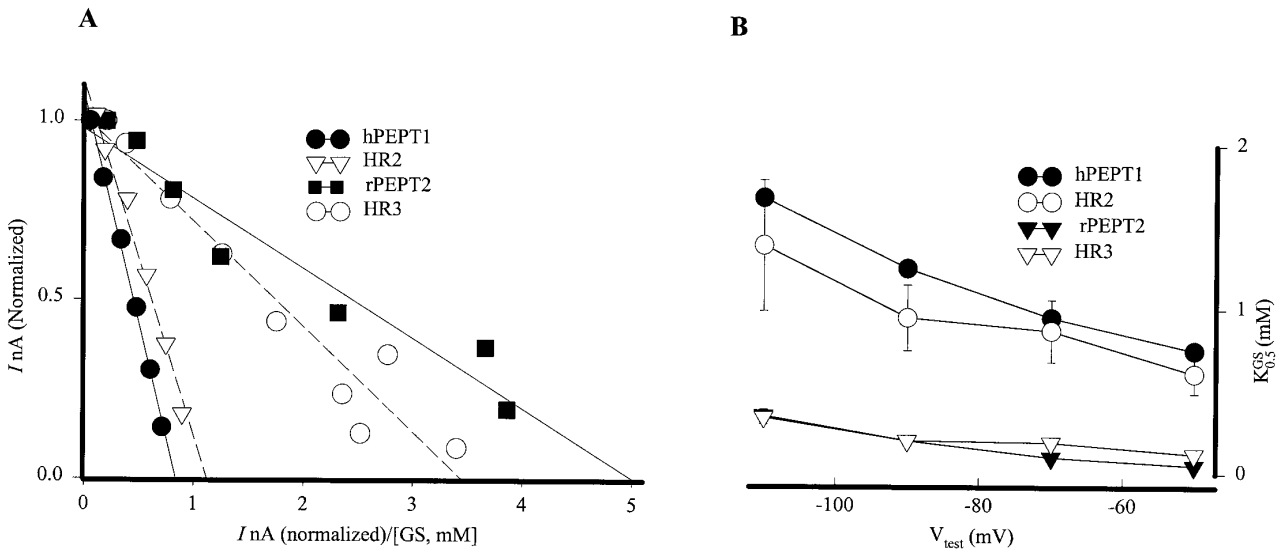

FIG. 3. Apparent affinities ($K^{GS}_{0.5}$) of chimeras HR2 and HR3 and the parental hPEPT1 and rPEPT2. A. Edie-Hofstee plots for the chimeric and parental transporters after normalization of the maximal current I_{max} to adjust for differences in the efficiency of expression in different oocytes. B. $K^{GS}_{0.5}$ of the chimeric and the parental transporters as a function of the testing membrane potential, V_{test}.

tials, chimera HR2 behaved like hPEPT1 and chimera HR2 behaved like rPEPT2 (Fig. 3B) with respect to substrate affinity. In all cases, the $K^{GS}_{0.5}$ value was found to be influenced by the testing membrane potential, the value becoming larger at hyperpolarizing membrane potentials. This characteristic was observed for all of the chimeras belonging to the low-affinity group and the high-affinity group (data not shown).

From these kinetic studies of the chimeras, it is apparent that substitution of the last $2\frac{1}{2}$ TMDs of hPEPT1 with the corresponding TMDs of rPEPT2 does not lead to any detectable change in substrate affinity. This is inferred from the findings that the $K^{GS}_{0.5}$ values for chimeras HR1 and HR2 are similar to the $K^{GS}_{0.5}$ value for hPEPT1. With respect to rPEPT2, substitution of the first $1\frac{1}{2}$ TMDs or the last $1\frac{1}{2}$ TMDs with the corresponding TMDs of hPEPT1 does not alter the substrate affinity. This is inferred form the data showing that the chimeras HR4, HR5, RH1 and RH2 behave like rPEPT2 with respect to substrate affinity.

The most interesting finding comes from the data obtained with chimeras HR2 and HR3. Chimera HR2 possesses the first $9\frac{1}{2}$ TMDs of hPEPT1 and the last $2\frac{1}{2}$ TMDs of rPEPT2. This chimera exhibits low-affinity for Gly-Sar similar to hPEPT1. Chimera HR3 possesses the first 6 TMDs of hPEPT1 and the last 6 TMDs of rPEPT2. This chimera, in contrast to chimera HR2, exhibits high-affinity for Gly-Sar similar to rPEPT2. Since the difference between the two chimeras lies in the region comprising the TMDs 7, 8 and the large extracellular loop between TMDs 9 and 10, this region seems to play a crucial role in the determination of the substrate affinity. If this particular region is derived from hPEPT1, the chimera behaves like hPEPT1 with low-affinity for Gly-Sar. On the other hand, if this region is derived from rPEPT2, the chimera behaves like rPEPT2 with high-affinity for Gly-Sar.

One of the most important differences with respect to the amino acid sequence of PEPT1 and PEPT2 is the large extracellular loop between M9 and M10. In this loop, the sequence identity was only 21% between PEPT1 and PEPT2. It may therefore seem that the differences in the characteristics of the PEPTs are likely to be associated with this loop. A recent study by Doring *et al* (19) has however shown that this extracellular loop is not a major determinant of the differential transport characteristics of PEPT1 and PEPT2. These investigators constructed a chimera, CH1Pep, using a restriction site dependent strategy. The chimera was composed of the N-terminal part from the rabbit PEPT2 (amino acid residues 1-401) and the C-terminal part from TMD 9 downwards including the loop between TMD 9 and 10 (amino acid residues 402-707) of the rabbit PEPT1. This chimera was found to behave like PEPT2, leading to the conclusion that the large extracellular loop between TMDs 9 and 10 does not play any significant role in determining the substrate affinity of PEPTs. The results from our present studies together with the results for the studies by Doring *et al* (19) suggest that the region in PEPT1 and PEPT2 comprising the TMDs 7, 8 and 9 with their in-between loops constitute the putative substrate binding site in these transporters.

Previous studies have shown that an obligatory histidyl residue (His-57 and His-87, in hPEPT1 and rPEPT2, respectively) is located near the extracellular

surface of the second putative transmembrane domain and that this residue plays an important role in the transport function of PEPTs (18, 20). Replacement of this essential histidyl residue by other amino acids results in a loss of the transport activity of PEPTs. Chemical modification of this histidyl residue can however be protected in the presence of peptide substrates (21, 22), even though chemical modification leads to a decrease in the maximal velocity of the transport process without affecting the affinity for peptide substrates (23). It is possible that this histidyl residue is located sterically close to the putative substrate binding site. Such proximity between the histidyl residue present near TMD2 and the putative substrate binding site present in the region consisting the TMDs 7, 8 and 9 is possible in the three dimensional topology of these transporters.

In summary, through a kinetic data analysis of the chimeric peptide transporters composed of different domains from the parental hPEPT1 and rPEPT2, we conclude that the putative substrate binding site in mammalian PEPTs resides in the region which is comprised of the TMDs 7, 8 and 9. This finding could be a first step towards a better understanding of the structure–function relationship in the case the mammalian peptide transporters and may have significant pharmacological relevance for the improvement in the design of peptidomimetic drugs.

ACKNOWLEDGMENT

This work was supported by National Institutes of Health Grant DK 28389.

REFERENCES

1. Ganapathy, V., and Leibach, F. H. (1991) *Curr. Opin. Cell Biol.* **3,** 695–701.
2. Leibach, F. H., and Ganapathy, V. (1996) *Annu. Rev. Nutr.* **16,** 99–119.
3. Ganapathy, V., and Leibach, F. H. (1996) *Curr. Opin. Nephrol. and Hyperten.* **5,** 395–400.
4. Fei, Y. J., Ganapathy, V., and Leibach, F. H. (1998) *Nucleic Acid Res. Mol. Biol.* **58,** 239–261.
5. Daniel, H. (1996) *J. Membrane Biol.* **154,** 197–203.
6. Fei, Y. J., Kanai, Y., Nussberger, S., Ganapathy, V., Leibach, F. H., Romero, M. F., Singh, S. K., Boron, W. F., and Hediger, M. A. (1994) *Nature* **368,** 563–566.
7. Boll, M., Markovich, D., Weber, W. M., Korte, H., Daniel, H., and Murer, H. (1994) *Pflugers Archiv- Eur. J. Physiol.* **429,** 146–149.
8. Liang, R., Fei, Y. J., Prasad, P. D., Ramamoorthy, S., Han, H., Yang-Feng, T. L., Hediger, M. A., Ganapathy, V., and Leibach, F. H. (1995) *J. Biol. Chem.* **270,** 6456–6463.
9. Liu, W., Liang, R., Ramamoorthy, S., Fei, Y. J., Ganapathy, M. E., Hediger, M. A., Ganapathy, V., and Leibach, F. H. (1995) *Biochim. Biophys. Acta* **1235,** 461–466.
10. Saito, H., Okuda, M., Terada, T., Dadaki, S., and Inui, K. (1995) *J. Pharmacol. Exp. Ther.* **275,** 1631–1637.
11. Boll, M., Herget, M., Wagener, M., Weber, W. M., Markovich, D., Biber, J., Clauss, W., Murer, H., and Daniel, H. (1996) *Proc. Natl. Acad. Sci. USA* **93,** 284–289.
12. Miyamoto, K., Shiraga, T., Morita, K., Yamamoto, H., Haga, H., Taketani, Y., Tamai, I., Sai, Y., Tsuji, A. and Takeda, E. (1996) *Biochim. Biophys. Acta* **1305,** 34–38
13. Saito, H., Terada, T., Okuda, M., Sasaki, S., and Inui, K. (1996) *Biochim. Biophys. Acta* **1280,** 173–177.
14. Moore, K. R., and Blakely, R. D. (1994) *BioTechniques* **17,** 130–136.
15. Buck, K. J., and Amara, S. G. (1994) *Proc. Natl. Acad. Sci. USA* 91, 12584–12588.
16. Sambrook, J., Fritsch, E. F., and Maniatis, T. (1989) Molecular Cloning: A Laboratory Manual. pp. 8.3–-8.82. Cold Spring Harbor Laboratory, New York.
17. Mackenzie, B., Loo, D. D. F., Fei, Y. J., Liu, W., Ganapathy, V., Leibach, F. H., and Wright, E. M. (1996) *J. Biol. Chem.* **271,** 5430–5437.
18. Fei, Y. J., Wei, L., Prasad, P., Kekuda, R., Oblak, T. G., Ganapathy, V., and Leibach, F. H. (1997) *Biochemistry* **36,** 452–460.
19. Doring, F., Dorn, D., Bachfischer, U., Amasheh, S., Herget, M., and Daniel, H. (1996) *J. Physiol.* **497,** 773–779.
20. Terada, T., Saito, H., Mukai, M., and Inui, K. (1996) *FEBS Letters* **394,** 196–200.
21. Miyamoto, Y., Ganapathy, V., and Leibach, F. H. (1986) *J. Biol. Chem.* **261,** 16133–16140.
22. Kato, M., Maegawa, H., Okano, T., Inui, K., and Hori, R. (1989) *J. Pharmacol. Exp. Ther.* **251,** 745–749.
23. Brandsch, M., Brandsch, C., Ganapathy, M. E., Chew, C. S., Ganapathy, V., and Leibach, F. H. (1997) *Biochim. Biophys. Acta* **1324,** 251–262.